Proceedings of the Eighth Meeting of the International Collaboration on Advanced Neutron Sources (ICANS-VIII)
8-12 July 1985, Rutherford Appleton Laboratory Report RAL-85-110

THE LOS ALAMOS CONSTANT-Q SPECTROMETER

R. A. Robinson, R. Pynn*, J. Eckert and J. A. Goldstone

Physics Division, Los Alamos National Laboratory, Los Alamos, N.M. 87545, U.S.A.

Abstract

A constant-Q spectrometer which has been installed on the pulsed source of the Los Alamos Neutron Scattering Center, is described. It features a number of innovations that ease sample and analyser alignment and a novel composite crystal analyser which exploits the mosaic properties of plastically deformed germanium in a new way. Observations of phonon dispersion in aluminium and of incoherent scattering in ZrH_2 are reported, along with background measurements.

1. Introduction

In this paper, we report the construction and initial operation of an improved constant-Q spectrometer[1] installed at the Los Alamos Neutron Scattering Center.[2] It is shown schematically in Figure 1 and its parameters are listed in Table 1. It is quite similar to the Harwell machine,[3,4] but features a number of significant improvements. Those relating to ease of operation of the instrument are listed in Section 2. In addition, we have proposed and tested a new analyser geometry, which is described in Section 3. In Section 4, we describe measurements on phonons in aluminium and we discuss data reduction. Finally, in Section 5, we outline our plans for future improvements and make some comments on pulsed

*Permanent address: Institut Laue Langevin, 156X Centre de Tri, 38042 Grenoble CEDEX, France

source inelastic instruments in general. We have chosen to emphasise new features or ideas in a fairly concise form and the reader interested in more detail is referred to Reference 1.

2. Improvements

(a) Line-up detector

We have chosen a longer sample-line-up detector flight path. This means that the Bragg peaks used in sample or analyser rocking curves are better separated. To boost count rate while searching for the peak in the first place, we have used a bank of three detectors subtending approximately 2°. In addition, vertical and horizontal ^{10}B-coated stretched film Soller collimators[5] (of 10' divergence) can be placed in this flight path for fine adjustment of sample or analyser orientation.

(b) Variable sample-image point separation

The spectrometer was constructed in such a way that the sample-image point separation can be varied between 20 and 40 cm. This entails moving the whole detector shielding assembly, which is mounted on rails, and moving the analyser crystal correspondingly. To this end, the analyser is suspended from a translation stage.

(c) Analyser mounting

The analyser crystal is mounted on a small two-axis motorised goniometer, which is in turn suspended from a two-dimensional translation stage. The idea of this arrangement is that the analyser can be translated reproducibly to the sample position (see A' in Figure 1) and that a rocking curve can be performed on the analyser, the scattered neutrons being detected in the same line-up counter as used for the sample. The analyser is then rotated (by 45°) and translated back to its normal position and orientation. We have experienced no difficulties aligning either samples or analyser crystals in this manner.

(d) Cadmium absorber after the sample

A major source of background is due to neutrons which pass directly through the sample, but which are then scattered, by air at the image point, directly into the main detector bank. To eliminate this source, we have placed a cadmium absorber in the beam midway between the sample and image points. This has the effect of reducing the subcadmium neutron background to better than 0.1 counts per minute. A typical background run is shown in Figure 2a. For comparison purposes, we also show a ZrH_2

spectrum in Figure 2b, and this Figure shows that it is possible to reach quite high energy transfers before background becomes a problem. We have also tried adding 3.5 mm of erbium, which has low energy nuclear resonances at 460 and 584 meV,[6] and this has the effect of moving the cut-off in Figure 2 to even shorter times. One could also consider using samarium and indium, which also have low-energy nuclear resonances, to push the threshold to yet shorter times.

(e) Other shielding arrangements

The shielding in the vicinity of the sample and analyser has been kept simple and flexible in order that the analyser can be moved and so that L_2 can be changed. When L_2 is at its minimum value, we have found it necessary to place vertical collimation between the sample and the analyser to eliminate contamination by out-of-plane analyser Bragg reflections. We have also placed 0.5 m long boron-aluminium composite sheets between the detectors as shown in Figure 1. These reduce the solid angle viewed by each detector and thereby reduce the background. An aluminium box, filled with B_4C, was placed behind the detector bank. In other respects, the spectrometer shielding was conventional.

3. The Analyser

Although we initially used a small germanium analyser (as described in Table 1) in the disc geometry proposed by Windsor,[4] we have proposed and tested an alternative, the "organ-pipe" geometry. It consists of a set of cylindrical crystals of identical crystallographic orientation, as shown in Figure 3. Any reflection in the [hhk] zone can be accessed by rotating all of the elements in unison. It has the following advantages:

(a) It maintains the flexibility of the disc (i.e., one can change reflection)

(b) It is far easier to make a large analyser in this geometry - less material is required and the cost is lower. This has the consequence that L_2 can be increased to provide room for sample environment equipment and collimators.

(c) The mosaic spread and thickness can be chosen to vary in the optimum manner along the length of the analyser (i.e., as a function of ϕ).

(d) The anisotropic mosaic properties of plastically deformed germanium (or copper) can be exploited to give a large mosaic spread within the

scattering plane (horizontal) and a small vertical mosaic spread for all reflections in the [hhk] zone. This is not possible in the disc geometry.

4. Results

As a demonstration experiment, we have chosen to measure several zone-boundary phonons in aluminium. We have exploited the fact that its lattice parameter is almost (to within 2.5%) exactly double the size of the (220) d-spacing of germanium. This means that one can scan along the zone boundary direction $\langle 1+\zeta, \bar{1}, 0\rangle$ as shown in the inset to Figure 4b. The results are shown as an intensity map in Figure 4a. There is clearly an intense, almost dispersionless phonon at approximately 25 meV, with a weaker dispersive mode at higher energies. Peak positions obtained from this map are compared to the 80 K results of Stedman and Nillson[7] in Figure 4b. The general agreement is good, but there is a small systematic discrepancy in the dispersive mode. This is mainly due to the fact that our measurements were made at room temperature and that the lattice is softer. A number of constant-$\underline{Q}$ scans can be constructed from these data and we show three in Figure 5. Resolution widths calculated within the framework reported previously[8,1] are also shown. In order to produce the intensity map shown in Figure 3a, the following steps must be followed:

(a) Perform rebinning from (ϕ,t) to $(Q_{\parallel},E)$ coordinates, where t is the observed time-of-flight, $Q_{\parallel}$ is the component of the momentum transfer parallel to the incident wave vector, and E is the energy transferred to the sample. This process should also include (implicitly or explicitly) multiplication by the appropriate Jacobian.

(b) Correct for the incident spectrum (which is measured using a low efficiency beam monitor), the detector efficiency and the analyser efficiency (the product of which can be measured in a vanadium scan).

(c) Correct for the variation of resolution volume across the data set. This is the equivalent of the $k_F^3 \cot\theta_A$ factor familiar in triple-axis spectroscopy.

5. Future Improvements

(a) More detectors

We are currently increasing the number of detectors to 64. It is clear from Figure 4a that the present number is insufficient, in the sense that one does not "get down to background" on both sides of the 25 meV phonon.

(b) Copper Analyser

We do not believe that second-order contamination is a problem in most experiments,[1] and one therefore does not need to use diamond structure material like germanium. We estimate[9] that gains of approximately 70% in reflectivity can be achieved at 50 meV if copper is used. The gain will be yet greater for higher incident energies. Furthermore, copper behaves in a more ideal manner during the plastic deformation process.

(c) Sample-analyser collimation

It would be advantageous to be able to vary the secondary spectrometer resolution using a fan-type collimator[10] between the sample and analyser. Backgrounds are also likely to be reduced once such a device is employed.

(d) Support the analyser crystal from below

The present arrangement is to mount the analyser crystal from above from a translation stage and to align it using the same line-up counter as for the sample. While this system poses no problems for small analysers, it is more difficult for large analyser assemblies. In addition, the supports for the translation stage get in the way of shielding and sample environment equipment for the sample. Given that we have shown that one can fabricate a large analyser crystal and thereby increase L_2 substantially, it may be worthwhile to support such an analyser from below, by means of a conventional goniometer. As it would no longer be possible to translate this to the sample position, a second line-up counter dedicated to the analyser would be necessary. Of course, it will still be necessary to translate it into the main beam for alignment purposes.

(e) Evacuate the image point

It will clearly be advantageous to evacuate the image point, or at least fill it with an argon atmosphere.

(f) Improve the moderator

As suggested at the Shelter Island Workshop,[11] this type of spectrometer could well benefit from a tall thin (vertically defocussed) moderator and one in which the moderator pulse width could be changed by means of a variable poison depth.

References

1. R. A. Robinson, R. Pynn and J. Eckert, submitted to Nucl. Instrum. Methods (1985) (also Los Alamos Report LAUR 85-1900).
2. R. N. Silver in Proceedings of 6th meeting of ICANS, Argonne,1982, Argonne National Laboratory Report ANL-82-80 p. 51.
3. C. G. Windsor, R. K. Heenan, B. C. Boland and D. F. R. Mildner, Nucl. Instrum. Methods 151, 477 (1978).
4. C. G. Windsor "Pulsed Neutron Scattering", Taylor and Francis, London 1981, Chapter 9.
5. C. J. Carlile, J. Penfold and W. G. Williams, J. Phys. E 11, 837 (1978)
6. S. F. Mughabghab and D. I. Garber, Brookhaven National Laboratory Report BNL-325, 3rd Edition, Volume I (1973).
7. R. Stedman and G. Nillson, Phys. Rev. 145, 492 (1966).
8. R. Pynn and R. A. Robinson, in Proceedings of Workshop on "High Energy Excitations in Condensed Matter" at Los Alamos, February 1984, Los Alamos Report LA-10227-C, p. 45.
9. For the method of calculation, see A. K. Freund in Proceedings of meeting on "Fokussierende Neutronenmonochromator und -analalysatoranordnungen", Hahn Meitner Institute Report HMI-B273 (1978) or R. A. Robinson and A. K. Freund, Institut Laue Langevin Report **** (1985).
10. A. F. Wright, M. Berneron and S. P. Heathman, Nucl. Instrum. Methods 180, 655 (1981).
11. C. G. Windsor, W. J. L. Buyers, R. A. Cowley, R. A. Robinson and S. M. Shapiro in Proceedings of Workshop on "Scientific Opportunities with Advanced Facilities for Neutron Scattering", Shelter Island, October 1984, CONF-8410256, p. 25.

TABLE 1

Moderator-sample distance L_1	6.990 m
Sample-image distance L_2	0.199-0.402 m
Image-detector distance L_3	1.447 m
Sample-alignment counter distance L_4	1.050 m
Angular (ϕ) range of detectors allowed by shielding	10°-70°
Spacing between detectors	0.59°
Moderator material	water at room temperature
thickness	2.3 cm
poisoning	none
area (viewed by sample)	~10 cm x 10 cm
Beam size at sample	2.5 cm wide x 5 cm high
Detectors	25x 1.25 cm diameter, 10 cm active length ^{3}He proportional counters, mounted vertically
Analysers	1x 5 cm diameter, 1 cm thick Ge disc and 1x 22cm long 5 cm high "organ-pipe" Ge analyser
Line-up detector	3 detectors identical to main detector
Incident beam monitor	1x low efficiency BF_3 monitor

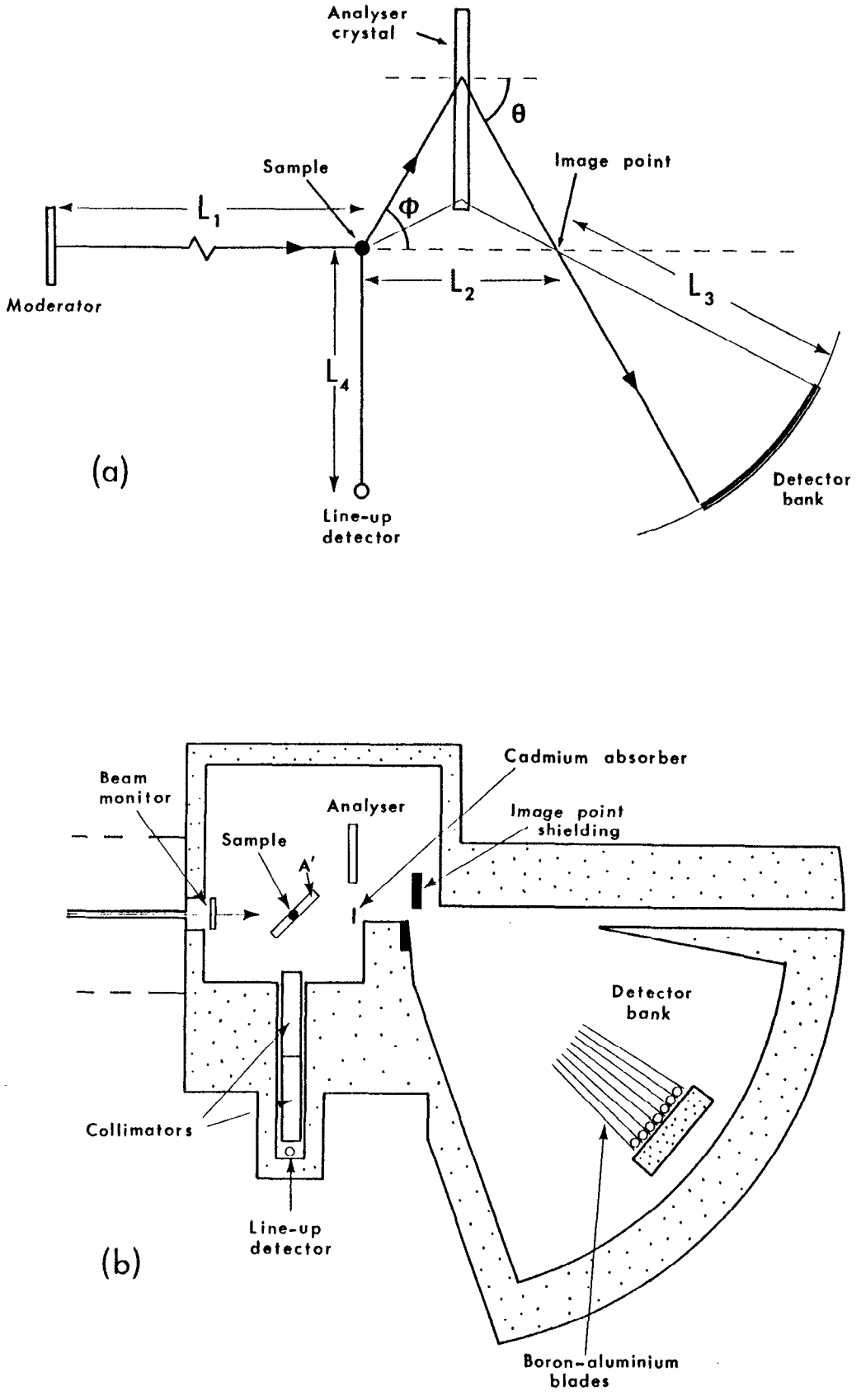

Figure 1: The schematic layout of a constant-Q spectrometer, showing (a) the symbolic conventions adopted in this work and (b) the physical details of the Los Alamos machine. A' = analyser translated to sample position for alignment purposes.

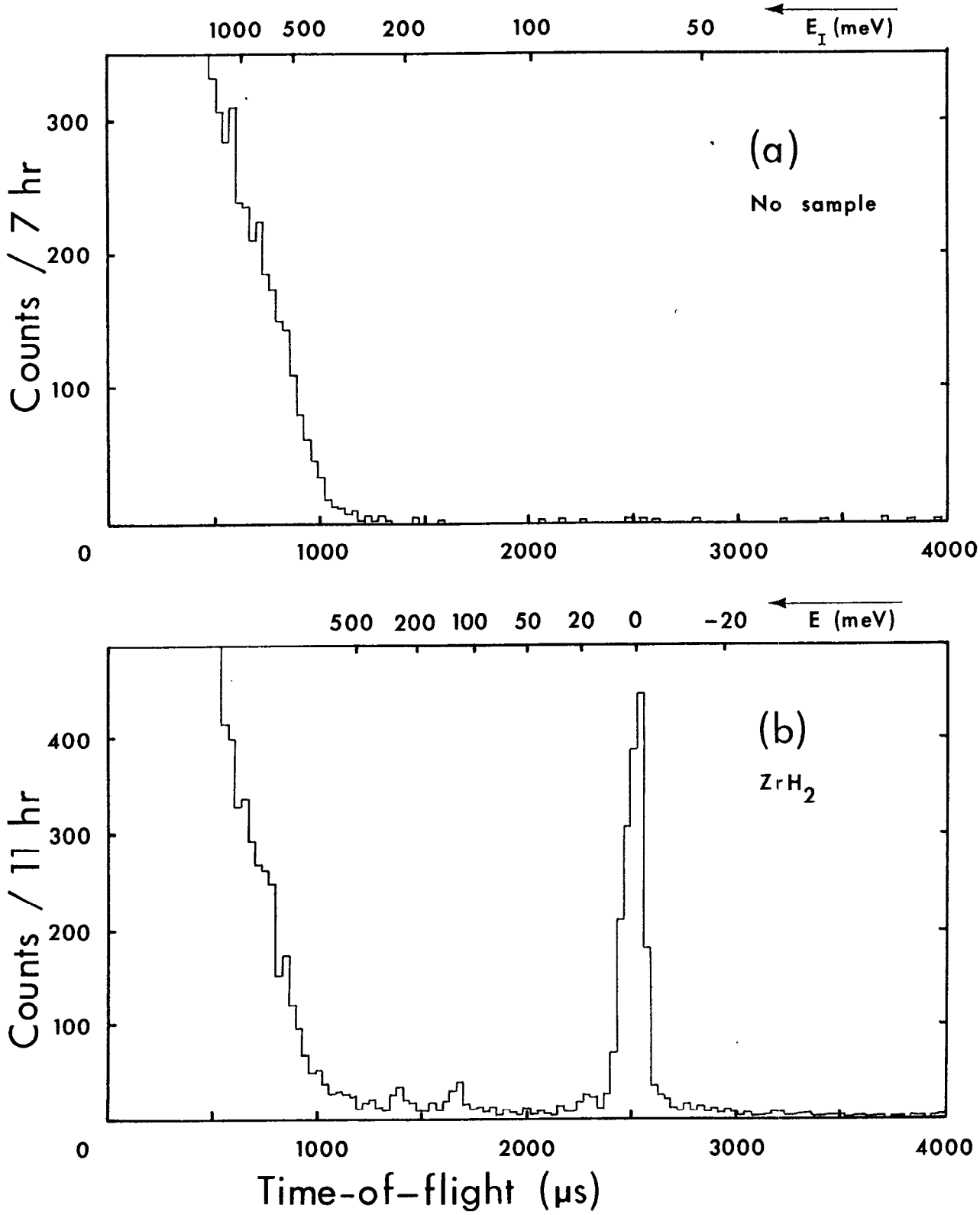

Figure 2: Time-of-flight spectra: (a) A background run. The spectrometer was set up with the "organ-pipe" analyser on the (331) reflection with no sample. ϕ = 24.5°. An energy scale, corresponding to elastic scattering at the image point is provided. (b) A ZrH_2 spectrum in the same counter as (a), with a Ge(331) analyser. An energy transfer scale is also provided. The elastic line is visible at 2500 μs and the first and second harmonics of the 140 meV excitation at 1700 and 1350 μs respectively. In both cases the data have been binned into 32 μs time channels.

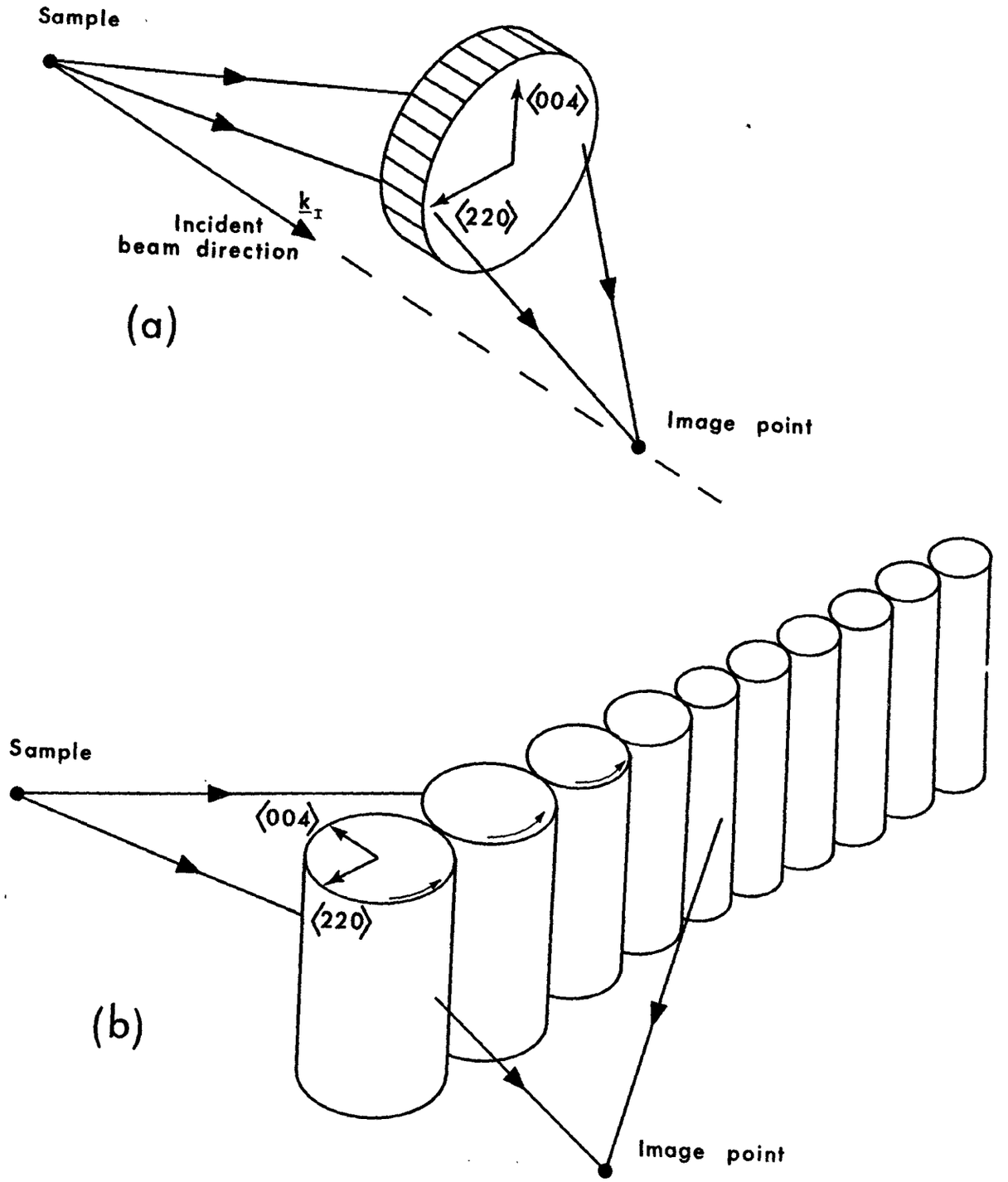

Figure 3: Possible flexible analyser geometries: (a) the disc[4] and (b) the "organ-pipe" described in detail in Reference 1.

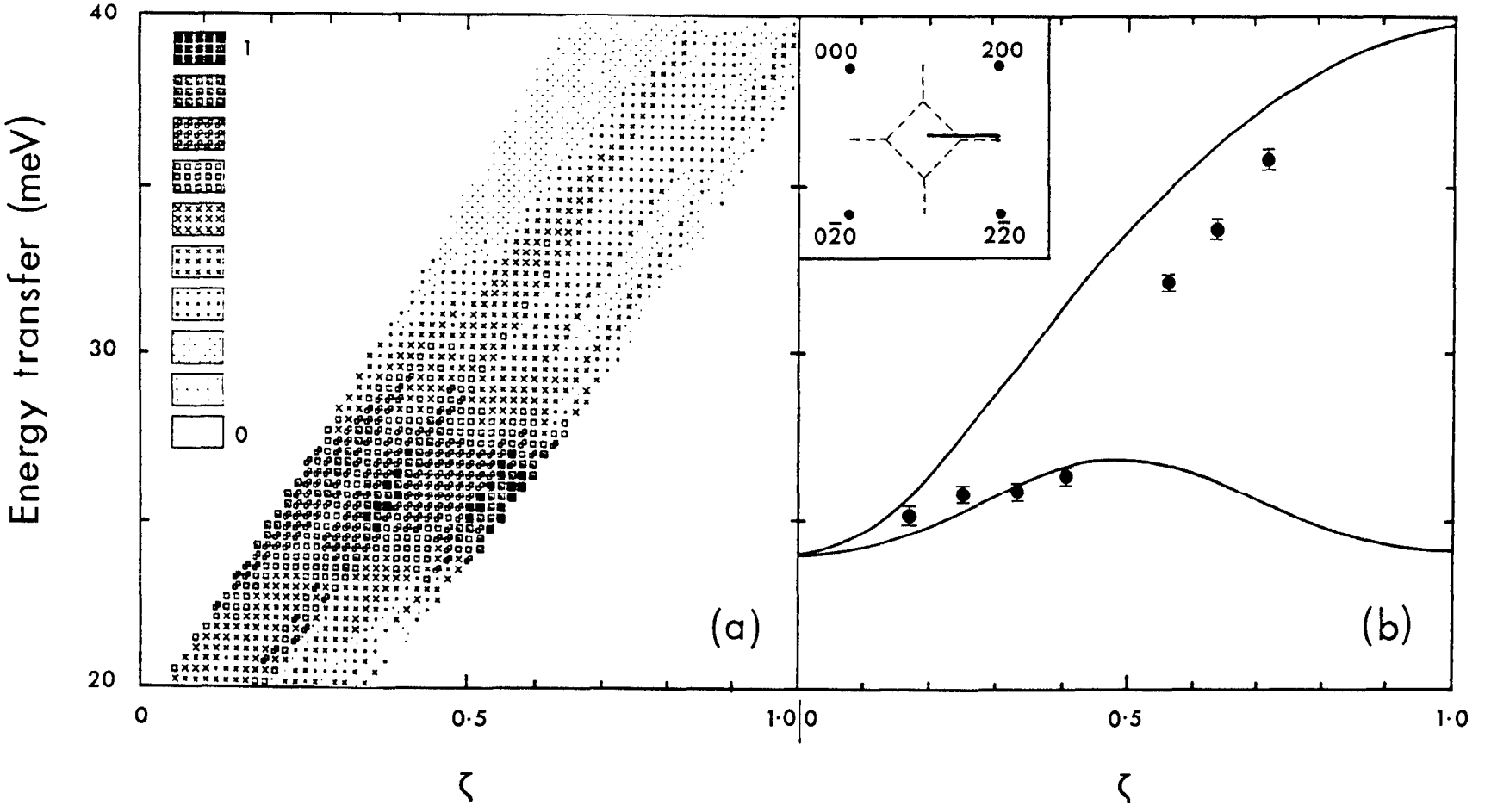

Figure 4: Aluminium phonon dispersion measured along $\langle 1+\zeta, \bar{1}, 0\rangle$ with a germanium (220) analyser: (a) our results presented as an intensity map and (b) dispersion curves for the same piece of $(Q_{\parallel}, E)$ space. The solid line represents the 80 K data of Stedman and Nillson[7] and the points show our results when binned into constant-Q scans. The vertical bars represent the errors in the positions of the respective constant-Q peaks. The measurements were made within the [001] zone, between $(1\bar{1}0)$ and $(2\bar{1}0)$ and this region of reciprocal space is shown in the inset. A quadratic intensity scale (from 0 to 1) was used, with 1 representing the intensity of the most intense $(Q_{\parallel}, E)$ bin.

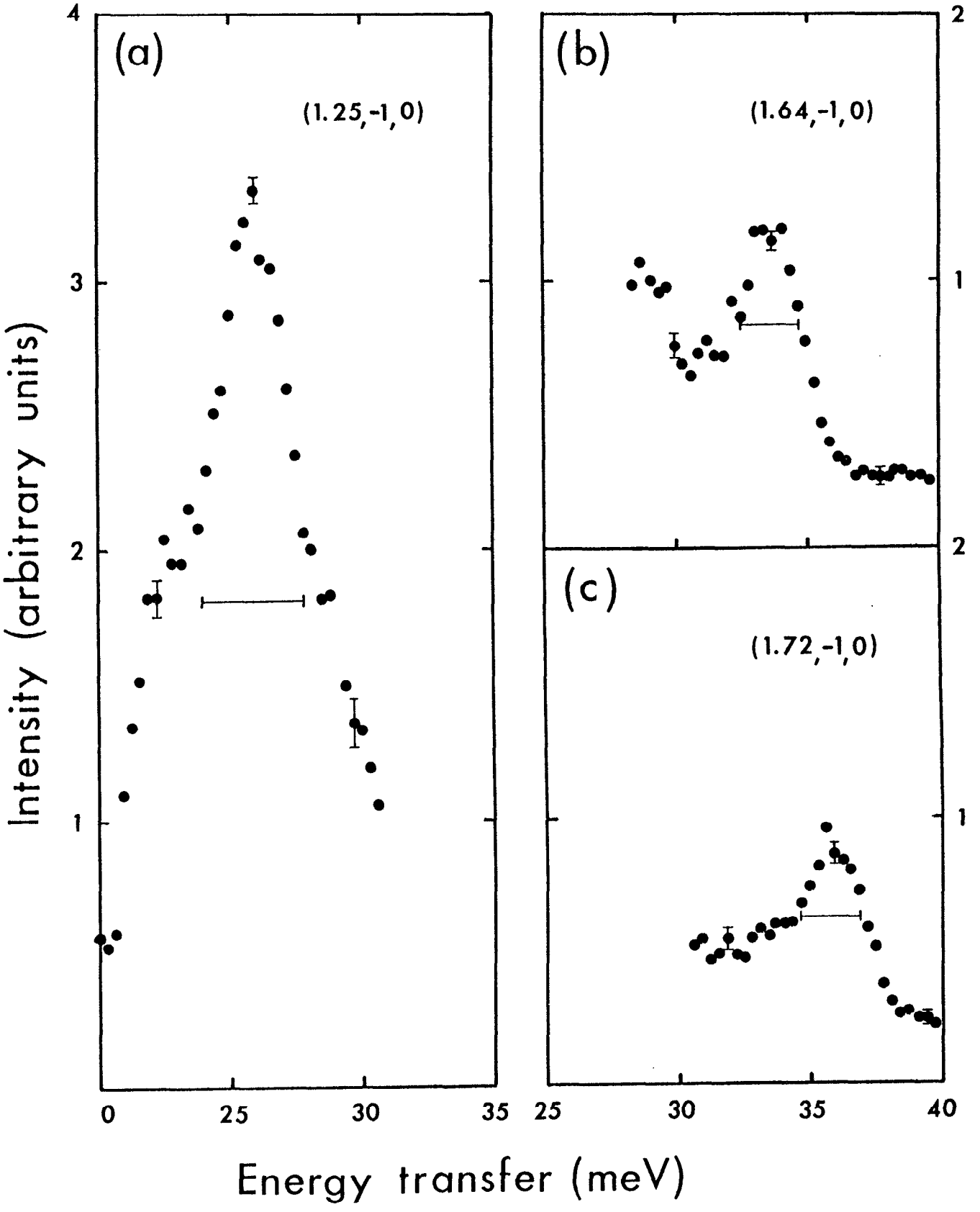

Figure 5: Constant-$\underline{Q}$ scans for (a) $\underline{Q}$ = (1.25,-1,0), (b) $\underline{Q}$ = (1.64,-1,0) and (c) $\underline{Q}$ = (1.72,-1,0) for aluminium at room temperature. Each scan was obtained by binning over 0.12Å^{-1} (0.078 reciprocal lattice units) in $Q_{\parallel}$. The horizontal bars show the calculated FWHM resolution width. The tail of the lower mode is clearly visible in (b), but there were not sufficient detectors at higher angles to cover this piece of $(Q_{\parallel},E)$ space.